BJR
© 2018 The Authors. Published by the British Institute of Radiology
https://doi.org/10.1259/bjr.20180507

Received: 05 June 2018 | Revised: 23 July 2018 | Accepted: 25 July 2018

Cite this article as:
Kim WH, Kim HJ, Lee SM, Cho SH, Shin KM, Lee SY, et al. Preoperative axillary nodal staging with ultrasound and magnetic resonance imaging: predictive values of quantitative and semantic features . *Br J Radiol* 2018; **91**: 20180507.

FULL PAPER

Preoperative axillary nodal staging with ultrasound and magnetic resonance imaging: predictive values of quantitative and semantic features

[1]WON HWA KIM, MD, [1]HYE JUNG KIM, MD, [1]SO MI LEE, MD, [1]SEUNG HYUN CHO, MD, [1]KYUNG MIN SHIN, MD, [1]SANG YUB LEE, MD, [1]JAE KWANG LIM, MD and [2]WON KEE LEE, PhD

[1]Department of Radiology, School of Medicine, Kyungpook National University, Kyungpook National University Chilgok Hospital, Daegu, South Korea
[2]Center of Biostatistics, School of Medicine, Kyungpook National University, Daegu, South Korea

Address correspondence to: Dr Hye Jung Kim
E-mail: *mamrad@knu.ac.kr*

Objective: Although axillary imaging has recently received renewed interest for preoperative staging in tandem with the evolving minimally invasive surgical approaches, axillary imaging is limited by the lack of standardization in the interpretation. We aimed to classify imaging features in ultrasound and MRI into quantitative and semantic features and evaluate predictive value of each feature for predicting nodal metastases.
Methods: A total of 316 breast cancers patients who underwent ultrasound and MRI prior to axillary surgery were included. Retrospective reviews of our breastimaging database were done for the quantitative features [cortical thickness (CT) and CT-derived parameters, long diameter (LD), short diameter (SD), and LD/SD ratio] and semantic features (eccentricity, loss of fatty hilum, and irregularity) of the axillary lymph node in images. Odd ratios (ORs) for each imaging feature were calculated with adjustment for clinicopathological characteristics significantly associated with nodal metastases.
Results: All CT-derived parameters were significantly associated with nodal metastases in both ultrasound and MRI (OR, 3.3–3.5 for ultrasound and 3.3–3.9 for MRI, respectively; Ps < .05). For the ultrasound, LD/SD ratio (OR, 2.1), eccentricity (OR, 2.4), and fatty hilum loss (OR, 27.2) were significantly associated with nodal metastases (Ps < .05). For the MRI, SD (OR, 2.1) and eccentricity (OR, 3.0) were significantly associated with nodal metastases (Ps < .05).
Conclusion: Among the quantitative features, all CT-derived parameters can be used for predicting nodal metastases. Significant predictors of semantic features were heterogeneous between ultrasound and MRI.
Advances in knowledge: (1) Imaging features of ultrasound and MRI for preoperative axillary nodal staging can be classified into quantitative and semantic features. (2) Predictive values of each imaging features are heterogeneous for predicting nodal metastases.

INTRODUCTION

The presence of metastases in axillary lymph nodes (ALNs) is a key determinant of prognosis in patients with breast cancer. Thus, surgical staging via sentinel lymph node biopsy (SLNB) or axillary lymph node dissection (ALND) is crucial in tailoring the treatment with adjuvant chemotherapy or radiotherapy.[1] Although the surgical exploration of the axillary lymph nodes is required for definitive staging, axillary imaging using ultrasound and MRI has recently received renewed interest for preoperative staging in tandem with the evolving minimally invasive approaches in the investigation of the axilla.[2–6] Researchers have been trying to identify a subgroup of patients with breast cancer that can avoid axillary surgery in the ongoing SOUND (Sentinel Node *vs* Observation after Axillary Ultrasound) and INSEMA (Intergroup Sentinel Mamma) trials.[7–10] In addition, following the results of the ACOSOG (American College of Surgeons Oncology Group) Z1011 and AMAROS trials, axillary imaging is also currently expected to identify patients who can be managed appropriately with SLNB alone or ALND and with or without radiation therapy.[11–13]

However, from a methodological standpoint, axillary imaging is limited by the lack of standardization in images acquisition and interpretation. In previous studies and clinical practice, many disorganized features, including cortical thickness (CT), size, morphology, and existence of fatty hilum, have been used to define a positive (abnormal or suspicious) ALN. However, the criteria for defining a

positive ALN vary among studies and institutions. Even for CT as a main determinant for positive ALN, consensus has not been achieved on how to measure CT and what threshold CT value indicates nodal metastases. Furthermore, the predictive value of each feature obtained from axillary imaging for nodal metastases remains unknown. Thus, in this study, we prospectively collected data for various features of axillary imaging, which were categorized as quantitative features [CT-derived parameters, long diameter (LD), short diameter (SD), and LD/SD ratio] and semantic features (irregularity, eccentricity, and fatty hilum loss). Then, retrospective analyses were performed to determine the optimum criteria of quantitative features and evaluate the predictive value of each semantic and quantitative feature. For obtaining CT-derived parameters, we proposed several methods, including difference in CT between ipsilateral (affected) and contralateral ALNs. These may improve the performance and reliability of axillary imaging. Herein, we aimed to classify imaging features in ultrasound and MRI into quantitative and semantic features and evaluate predictive value of each feature for predicting nodal metastases.

METHODS AND MATERIALS

Study population

This retrospective analysis of prospectively maintained database was approved by our institutional review board, and the requirement for informed consent was waived. A review of the breast-imaging database of Kyungpook National University Chilgok Hospital identified 451 patients with invasive breast cancer who underwent breast and axillary surgery between December 2016 and November 2017. We excluded females who underwent neoadjuvant chemotherapy (n = 80), had excisional or vacuum-assisted biopsy before surgery (n = 42), and had synchronous bilateral breast cancers (n = 13). Therefore, 316 patients were included in this study. Their mean age at diagnosis was 53 years (range, 23–85 years).

Image acquisition and analysis

Two breast imaging radiologists (HJKand WHK, with 18 and 10 years of experience, respectively) performed bilateral whole-breast and axillary ultrasound examinations and interpreted ultrasound and MRI images prior to surgery. Ultrasound was performed using an iU22 system (Philips-Advanced Technology Laboratories, Bothell, WA) equipped with 50 mm L12–5 MHz transducer and Aixplorer system (SuperSonic Imagine, Aix en Provence, France) equipped with a 50 mm SL15-4 MHz transducer. Patients were placed in the supine or supine oblique position, with the arm raised above the head and abducted. The radiologists examined carefully the entire axillary region at the levels I–III and found the most suspicious ALN with the thickest cortex in each (affected and contralateral) axilla. The radiologists assessed semantic features of the ALN (irregularity, eccentricity, and fatty hilum loss) and measured the quantitative features (CT of ipsilateral and contralateral ALNs, LD and SD of ipsilateral ALN). These features were documented in our breast-imaging database. For CT measurement, they identified the thickest cortical area, except at the vertex area, in the plane of the ALN where the fatty hilum is most visible (Figure 1a,b). If the ALN had loss of fatty hilum, CT was measured by two ways: radius (CT^R) and SD (CT^D) (Figure 1c).

Breast MRI was performed with the patient prone using a 3.0 T system (Discovery MR750, GE Healthcare, Waukesha, WI)

Figure 1. Diagram shows CT measurement used in this study. CT was measured at the thickest area of the cortex (a), except at the vertex area, in the plane of the ALN where the fatty hilum was most visible. If the ALN had eccentricity (b), CT was measured at the most eccentric cortical thickening. Diagram (c) shows CT measurement for the ALN with fatty hilum loss. CT was measured using two parameters: radius (CT^R) and short diameter (CT^D). ALN, axillary lymph node; CT, cortical thickness.

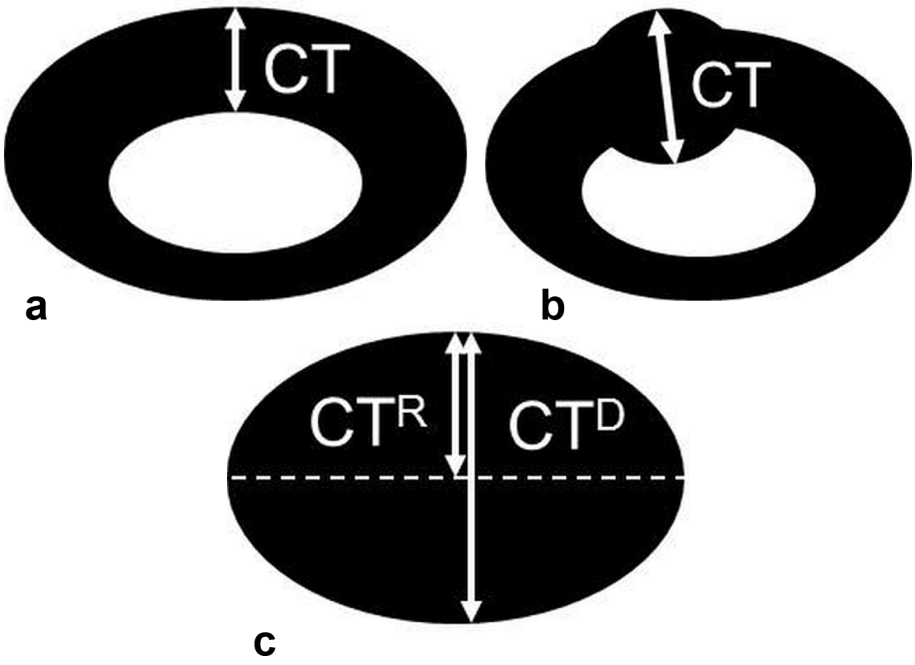

Table 1. Clinicopathological characteristics of patients with benign and metastatic axillary lymph nodes

Variables	Total (n = 316)	Benign (n = 226)	Metastatic (n = 90)	p-value
Histologic type				.444
Invasive ductal	292 (92.4%)	206 (91.2%)	86 (95.6%)	
Invasive lobular	12 (3.8%)	9 (4.0%)	3 (3.3%)	
Metaplastic	2 (0.6%)	2 (0.9%)	0 (0.0%)	
Mucinous	10 (3.2%)	9 (4.0%)	1 (1.1%)	
T stage				<.001
T_1	239 (75.6%)	189 (83.6%)	50 (55.6%)	
T_2	75 (23.7%)	37 (16.4%)	38 (42.2%)	
T3	2 (0.6%)	0 (0.0%)	2 (2.2%)	
Age				1.00
≤50 years	158 (50.0%)	113 (50.0%)	45 (50.0%)	
>50 years	158 (50.0%)	113 (50.0%)	45 (50.0%)	
Tumor location				.036
Others[a]	148 (46.8%)	116 (51.3%)	32 (35.6%)	
Upper outer	153 (48.4%)	101 (44.7%)	52 (57.8%)	
Subareolar	15 (4.7%)	9 (4.0%)	6 (6.7%)	
Histologic grade				.025
Low	34 (10.8%)	31 (13.7%)	3 (3.3%)	
Moderate	192 (60.8%)	134 (59.3%)	58 (64.4%)	
High	90 (28.5%)	61 (27.0%)	29 (32.2%)	
HR status				.986
Negative	63 (19.9%)	45 (19.9%)	18 (20.0%)	
Positive	253 (80.1%)	181 (80.1%)	72 (80.0%)	
HER2 status[b]				.489
Negative	236 (80.8%)	166 (79.8%)	70 (83.3%)	
Positive	56 (19.2%)	42 (20.2%)	14 (16.7%)	

HER2, human epidermal growth factor receptor; HR, hormone receptor.
Data are the numbers of patients, with percentages.
[a]Other locations include upper inner, lower outer, and lower inner quadrants.
[b]Limited to patients with available data only (n = 292).

with a dedicated 8-channel surface breast coil. Each patient was administered 0.1 ml kg^{-1} of gadobutrol (Gadovist, Bayer Schering Pharma, Berlin, Germany) as the contrast agent, which was injected at a rate of 1 ml s^{-1}. Axial T_1 weighted images [repetition time/echo time (TR/TE), 746/10; matrix, 352 × 256; slice thickness, 3 mm] and axial fat-suppressed T_2 weighted images (TR/TE, 8087/88; matrix, 384 × 256; slice thickness, 3 mm) were acquired. Dynamic contrast-enhanced MR examination included one pre-contrast and five post-contrast imaging with bilateral axial acquisition using three-dimensional gradient-echo fat-suppressed T_1 weighted imaging (TR/TE, 4/2; matrix, 288 × 416; flip angle, 15°; slice thickness, 1 mm). For evaluation of ALN, measurement of the quantitative features (CT, LD, and SD) and determination of the semantic features (irregularity, eccentricity, and fatty hilum loss) were conducted in the same way as ultrasound examinations. At breast MRI, measurements of CT, LD, and SD were performed using the non-enhanced, fat-suppressed T_1 weighted images to avoid errors due the hilar vascular density caused by contrast enhancement.

Reference of standard

All suspicious ALNs those were determined by the radiologists were aspirated using fine-needle aspiration or removed during axillary surgery after tattooing. For fine-needle aspiration, a 23-gauge needle was inserted into the cortex of the ALN using a to-and-fro method with manual aspiration. Tattooing of the aspirated ALNs was performed by injection of 1 to 3 ml of CharcotraceTM black ink (Phebra, Lane Cove West, Australia) into the cortex of ALNs and the adjacent soft tissue. All patients underwent SLNB and/or ALND for axillary nodal staging. ALNs were examined using hematoxylin and eosin staining. Each ALN was classified as negative or positive for metastases. All

Table 2. Overall diagnostic performance of ultrasound and MRI features for diagnosis of nodal metastases

Variables	Cut-off Value	AUC (95% CI)	*p*-value
Ultrasound (n = 316)			
CT^{R}[a]	>2.3 mm	0.635 (0.579 to 0.688)	<.001
CT^{D}[a]	>2.3 mm	0.642 (0.586 to 0.694)	<.001
CT-bilateral difference^{R}[b]	>0.7 mm	0.656 (0.601 to 0.709)	<.001
CT-bilateral difference^{D}[b]	>0.7 mm	0.662 (0.607 to 0.714)	<.001
LD	≤13 mm	0.542 (0.486 to 0.598)	.234
SD	>4.5 mm	0.532 (0.475 to 0.588)	.380
LD/SD	≤1.7	0.557 (0.501 to 0.613)	.110
Eccentricity	N/A	0.565 (0.508 to 0.620)	.010
Fatty hilum loss	N/A	0.548 (0.491 to 0.604)	.003
Irregularity	N/A	0.512 (0.456 to 0.569)	.442
MRI (n = 260)			
CT^{R}[a]	>3.0 mm	0.622 (0.560 to 0.681)	.004
CT^{D}[a]	>3.0 mm	0.632 (0.570 to 0.690)	.002
CT-bilateral difference^{R}[b]	>0.8 mm	0.647 (0.586 to 0.705)	<.001
CT-bilateral difference^{D}[b]	>0.8 mm	0.651 (0.589 to 0.708)	<.001
LD	>10 mm	0.560 (0.497 to 0.621)	.132
SD	>5.9 mm	0.588 (0.526 to 0.649)	.032
LD/SD	≤2.8	0.533 (0.470 to 0.595)	.412
Eccentricity	N/A	0.587 (0.525 to 0.648)	.003
Fatty hilum loss	N/A	0.532 (0.469 to 0.594)	.131
Irregularity	N/A	0.527 (0.465 to 0.589)	.171

AUC, area under the receiver operating characteristic curve; CT, cortical thickness; LD, long diameter; SD, short diameter.
[a]If the ALN had loss of fatty hilum, two CT features were assessed: radius (CT^{R}) or SD (CT^{D}).
[b]CT-bilateral difference^{R} was calculated by CT^{R} minus CT of contralateral ALN and CT-bilateral difference^{D} by CT^{D} minus CT of contralateral ALN.

histopathological evaluations were performed by two pathologists (JYP and JYJ with 18 and 10 years of experience in breast pathology, respectively).

Data collection and statistical analysis

The following clinicopathological information was included: histologic type, T stage, age, histologic grade, and estrogen receptor (ER), progesterone receptor (PR), and human epidermal growth factor receptor 2 (HER2) statuses. The expression of ER, PR, and HER2 was assessed by immunohistochemical staining. The expression of ER and PR was quantified using the Allred score: a total Allred score of >2 was considered as positive for ER or PR.[14] A HER2 score of 0 or 1 was considered negative (HER2-negative), a value of 3 was considered positive (HER2-positive), and value of 2 was considered equivocal. For equivocal cases, silver-enhanced *in situ* hybridization was performed, and a HER2/CEP17 ratio of ≥2 or HER2/CEP17 ratio of <2 with an average HER2 copy number of ≥6 were considered positive (HER2-positive).[15] Hormone receptor-positive status was defined as tumors expressing ER and/or PR. The clinicopathological characteristics of patients with benign and metastatic ALN were compared using a X^2 test.

For imaging features with ultrasound, the following quantitative features were assessed: CT^{R}, CT^{D}, CT-bilateral difference^{R} (CT^{R} minus CT of the contralateral ALN), CT-bilateral difference^{D} (CT^{D} minus CT of the contralateral ALN), LD, SD, and LD/SD. For these quantitative features, the optimum cut-off values for predicting nodal metastases were independently determined using the receiver operating characteristic (ROC) analysis; the best Youden index (sensitivity +specificity − 1) was used. The overall diagnostic performance was estimated by calculating the area under the ROC curve (AUC) with 95% confidence interval and *p*- value. For the calculation of odds ratios (ORs) with 95% confidence intervals, the quantitative features were divided into binary groups according to each cut-off value. The ORs for predicting nodal metastases were calculated using univariate logistic regression analysis, and adjusted ORs were calculated using the multivariate logistic regression model with the clinicopathological characteristics that were statistically associated with nodal metastases. All statistical analyses were performed with the statistical software SPSS v. 24.0 (Chicago, IL) and MedCalc v. 17.1 (Mariakerke, Belgium). Two-tailed *p*-values of less than.05 were considered statistically significant.

Figure 2. Ultrasound images of a 73-year-old female with a breast cancer in her right breast. Cortical thickness was measured as 4.2 mm in the ipsilateral (a) and as 1.3 mm in the contralateral ALN (b). Ipsilateral ALN had nodal metastases in ultrasound-guided aspiration with subsequent surgical resection. ALN, axillary lymph node.

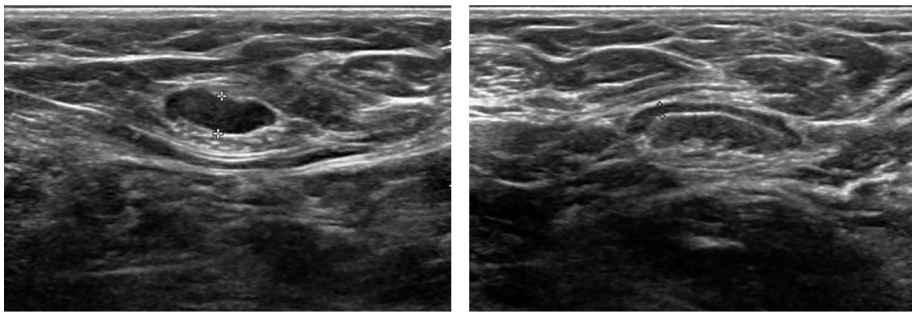

RESULTS

Clinicopathological characteristics in patients with benign and metastatic ALN are summarized in Table 1. Of the 316 patients, 226 (71.5%) had benign ALN and 90 (28.5%) had metastatic ALN based on the surgical histopathological results. Patients with metastatic ALN had tumors with higher T stages ($p < .001$) and higher histologic grades ($p = .025$). Tumors located in the upper outer quadrant or subareolar area were more frequently found in patients with metastatic ALN than in patients with benign ALN ($p = .036$).

Table 2 shows the overall diagnostic performances of each imaging feature in ultrasound and MRI and the optimum cut-off values for the measurements. With respect to the ultrasound, the mean CT^R and CT^D of the affected ALN were 1.9 mm (range, 0.1–7.0 mm) and 2.1 mm (range, 0.1–11.0 mm), respectively. The mean CT of the contralateral ALN was 1.4 mm (range, 0.3–3.5 mm). The mean CT-bilateral difference was 0.5 mm (range, −1.3 to 5.5 mm) and 0.6 mm (range, −1.3 to 9.5 mm), respectively for CT-bilateral difference^R and CT-bilateral difference^D. The optimum cut-off value was >2.3 mm for both CT^R and CT^D and >0.7 mm for both CT-bilateral difference^R and CT-bilateral difference^D. The AUC of CT-bilateral difference^D (0.662) was the largest, whereas the other CT-derived parameters (CT^R, CT^D, and CT-bilateral difference^R) showed AUCs ranging from 0.635 to 0.656 (Figure 2). With respect to MRI, the mean CT^R and CT^D of the affected ALN were 2.3 mm (range, 0.7–7.3 mm) and 2.6 mm (range, 0.7–16.0 mm), respectively. The mean CT of the contralateral ALN was 1.6 mm (range, 0.9–4.0 mm). The mean CT-bilateral difference was 0.7 mm (range, −1.2 to 5.6 mm) and 1.0 mm (range, − 1.2 to 16.0 mm), respectively for CT-bilateral difference^R and CT-bilateral difference^D. The optimum cut-off value was >3.0 mm for both CT^R and CT^D and >0.8 mm for both CT-bilateral difference^R and CT-bilateral difference^D. The AUC of CT-bilateral difference^D (0.651) was the highest, whereas the other CT-derived parameters (CT^R, CT^D, and CT-bilateral difference^R) showed AUCs ranging from 0.622 to 0.647.

ORs for each imaging features associated with nodal metastases are shown in Table 3. Adjusted ORs (adjusted for T stage, tumor location, and histologic grade) that were significantly associated with nodal metastases (Table 1) are also shown. All CT-derived parameters were significantly associated nodal metastases with adjusted ORs ranging from 2.9 to 3.5 and 3.3 to 4.0 in ultrasound and MRI, respectively. With respect to ultrasound, LD/SD ratio, eccentricity, and fatty hilum loss were significantly associated with nodal metastases. Fatty hilum loss had the greatest OR of 27.2 for nodal metastases. LD, SD, and irregularity were not significantly associated with nodal metastases. With respect to MRI, SD and eccentricity were significantly associated with nodal metastases (Figure 3). CT-bilateral difference^D had the greatest OR of 4.0 for nodal metastases. LD, LD/SD, fatty hilum loss, and irregularity were not significantly associated with nodal metastases.

DISCUSSION

Although the role and performance of preoperative imaging of the axilla has been substantially evaluated, there is still wide variability in the criteria used to define a positive ALN, and the need for standardization of the criteria has been continuously recognized. Among the various imaging features, increased CT is considered to be the main feature that is indicative of metastatic changes; this is because the metastatic cells are located first in the cortex of a node.[16,17] In this study, we present methods how to measure CT in ALN and our results indicate that all CT-derived parameters can be used for predicting nodal metastases. For the ALN with fatty hilum loss, it is not specified to measure CT. In our study, CT was measured by two ways: using the radius (CT^R) and diameter (CT^D) of the ALN with fatty hilum loss. We found that both measurements of CT^R and CT^D were generally similar in the overall diagnostic performance and predictive value. In addition, since CT is known to vary among individuals and bilateral comparison of CT has not been examined to date, we also evaluated the differences in CT (ipsilateral–contralateral) for predicting nodal metastases.[18] Our results showed that the optimum cut-off value for bilateral comparison was >0.7 mm in ultrasound and >0.8 mm in MRI. In addition, the maximum AUC for predicting nodal metastases was achieved by CT-bilateral difference^D in ultrasound and MRI. This suggests that bilateral comparison of CT is more useful than CT itself for predicting nodal metastases. With respect to normal range of CT, findings of a current study using MRI suggests that the mean value of normal CT for black and Caucasian females was 3.3 mm and 2.6 mm, respectively.[18] In our study with Asian females,

Table 3. ORs for imaging features associated with nodal metastases

Variables	OR	*p*-value	Adjusted OR[c]	*p*-value[c]
Ultrasound (*n* = 316)				
CT^{R}[a]	3.6 (2.1 to 6.3)	<.001	3.5 (1.9 to 6.3)	<.001
CT^{D}[a]	3.6 (2.1 to 6.3)	<.001	3.3 (1.8 to 5.9)	<.001
CT-bilateral difference^{R}[b]	3.4 (2.0 to 5.7)	<.001	3.0 (1.7 to 5.4)	<.001
CT-bilateral difference^{D}[b]	3.4 (2.0 to 5.8)	<.001	2.9 (1.6 to 5.1)	<.001
LD	1.7 (1.0 to 2.7)	.047	1.6 (1.0 to 2.8)	.069
SD	1.4 (0.8 to 2.4)	.187	1.4 (0.8 to 2.5)	.249
LD/SD	2.2 (1.2 to 4.2)	.012	2.1 (1.1 to 4.2)	.032
Eccentricity	2.5 (1.3 to 4.7)	.005	2.4 (1.2 to 4.8)	.011
Fatty hilum loss	25.0 (3.1 to 200.4)	.002	27.2 (2.7 to 269.2)	.005
Irregularity	1.5 (0.6 to 4.0)	.408	1.9 (0.7 to 5.5)	.231
MRI (*n* = 260)				
CT^{R}[a]	3.7 (2.0 to 6.8)	<.001	3.3 (1.7 to 6.7)	.001
CT^{D}[a]	4.0 (2.2 to 7.4)	<.001	3.9 (2.0 to 7.7)	<.001
CT-bilateral difference^{R}[b]	4.2 (2.3 to 7.6)	<.001	3.7 (1.9 to 7.2)	<.001
CT-bilateral difference^{D}[b]	4.3 (2.4 to 7.7)	<.001	4.0 (2.1 to 7.7)	<.001
LD	1.8 (1.0 to 3.1)	.045	1.8 (1.0 to 3.3)	.053
SD	2.3 (1.3 to 4.0)	.004	2.1 (1.2 to 3.9)	.015
LD/SD	2.8 (0.9 to 8.3)	.064	2.7 (0.9 to 8.3)	.088
Eccentricity	3.1 (1.6 to 6.2)	.001	3.0 (1.4 to 6.3)	.004
Fatty hilum loss	2.4 (0.9 o 6.3)	.082	1.9 (0.7 to 5.4)	.241
Irregularity	2.3 (0.8 to 6.4)	.116	1.8 (0.6 to 5.6)	.322

CT, cortical thickness; LD, long diameter; OR, odds ratio; SD, short diameter.
For the calculation of OR, quantitative features (CT^{R}, CT^{D}, CT-bilateral difference^{R}, CT-bilateral difference^{D}, LD, SD, LD/SD) were divided into binary groups according to each cut-off value.
[a]If the ALN had loss of fatty hilum, two CT features were assessed: radius (CT^{R}) or SD (CT^{D}).
[b]CT-bilateral difference^{R} was calculated by CT^{R} minus CT of contralateral ALN and CT-bilateral difference^{D} by CT^{D} minus CT of contralateral ALN.
[c]Adjusted for T stage, tumor location, and histologic grade.

the mean value of normal CT was 1.6 mm (range, 0.9–4.0 mm) on MRI and 1.4 mm (range, 0.3–3.5 mm) on ultrasound. The values observed in our study seemed to be lower than the values observed in a previous study; this may be attributed to racial differences. With respect to MRI, there has been a report that indicated asymmetry in the overall pattern the ALNs in the axilla is also a significant predictor for nodal metastases.[19] However, in our study, we did not consider the overall pattern of ALNs, but rather we focused on the most suspicious ALN.

The cut-off values of CT for ALN positivity have varied among studies, and they have generally been within the range of 2.0–3.0 mm.[20–24] In this study using ROC analysis of a large series of patients, we found that a CT of >2.3 mm was the optimum cut-off value for ultrasound. We also found that the cut-off value for MRI was >3.0 mm, which was higher than cut-off value for ultrasound. This difference is probably related to the trade-off between image resolution and field of view (FOV); a higher FOV of an MRI may preclude an accurate differentiation of the inner margin of the cortex from the fatty hilum due to a lower image resolution, and this can potentially overestimate the CT. The difference may also be due to the inherent characteristics of ultrasound and MRI; real-time ultrasound imaging allows the ALN to be viewed in a major axis where the fatty hilum is most visible, whereas sectional imaging using MRI with predetermined slice thickness and scan axis does not allow for viewing of the major axis.

In this study, we found that predictive values of each feature were dissimilar between ultrasound and MRI. With respect to the quantitative features, all CT-derived parameters showed significant association with nodal metastases in both ultrasound and MRI. LD/SD ratio in ultrasound was significantly associated with nodal metastases, whereas LD/SD ratio in MRI was not significantly associated with nodal metastases; on the contrary, SD was significantly associated with nodal metastases in MRI. Because the size of ALN is considered to be variable, ALN positivity is not generally determined according to its LD.

Figure 3. MR images of a 47-year-old female with breast cancer in her right breast. Axial non-enhanced, fat-suppressed T_1 weighted images (a–d) show ipsilateral (a, arrow) and contralateral (b, arrow) ALNs. Ipsilateral ALN had a cortical thickness of 5.5 mm (c) and its short diameter was 8.6 mm (d). The contralateral ALN (d) had a cortical thickness of 1.6 mm and its short diameter was 3.4 mm. Ultrasound-guided aspiration of the ipsilateral ALN with subsequent surgical resection revealed nodal metastases. ALN, axillary lymph node.

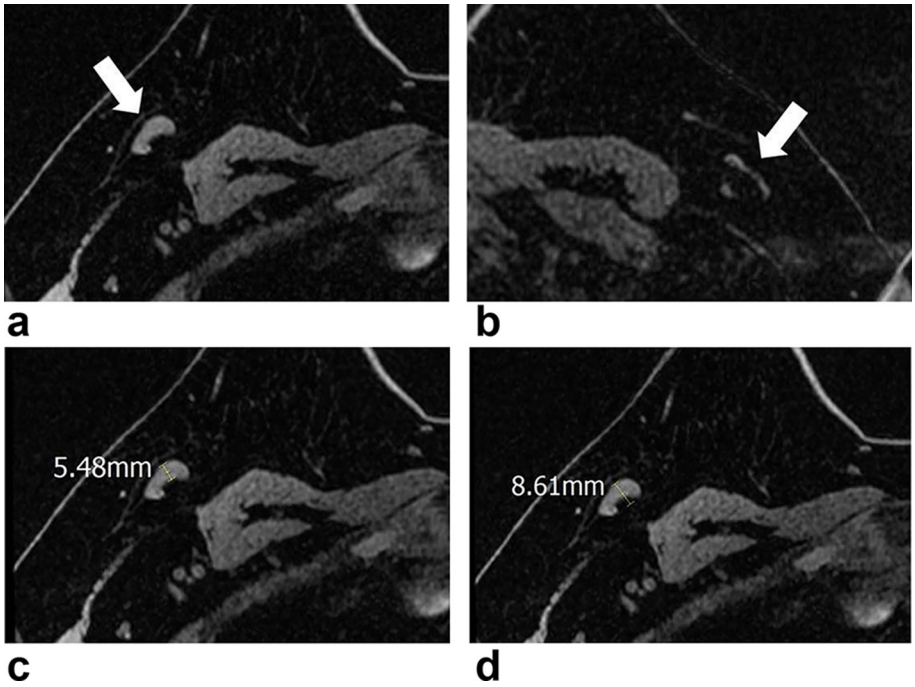

Figure 4. MR and ultrasound images of a 66-year-old female with breast cancer in her right breast. Axial non-enhanced, fat-suppressed T_1 weighted image (a) and T_2 weighted image (b) shows ipsilateral ALN (arrow) without obvious fatty hilum. Ultrasound image of the ipsilateral ALN (c) with scanty amount of fatty hilum (arrow) and its cortical thickness was 2.0 mm. Cortical thickness of the contralateral ALN (d) was 1.5 mm. This patient had no nodal metastases in the surgical specimen. ALN, axillary lymph node.

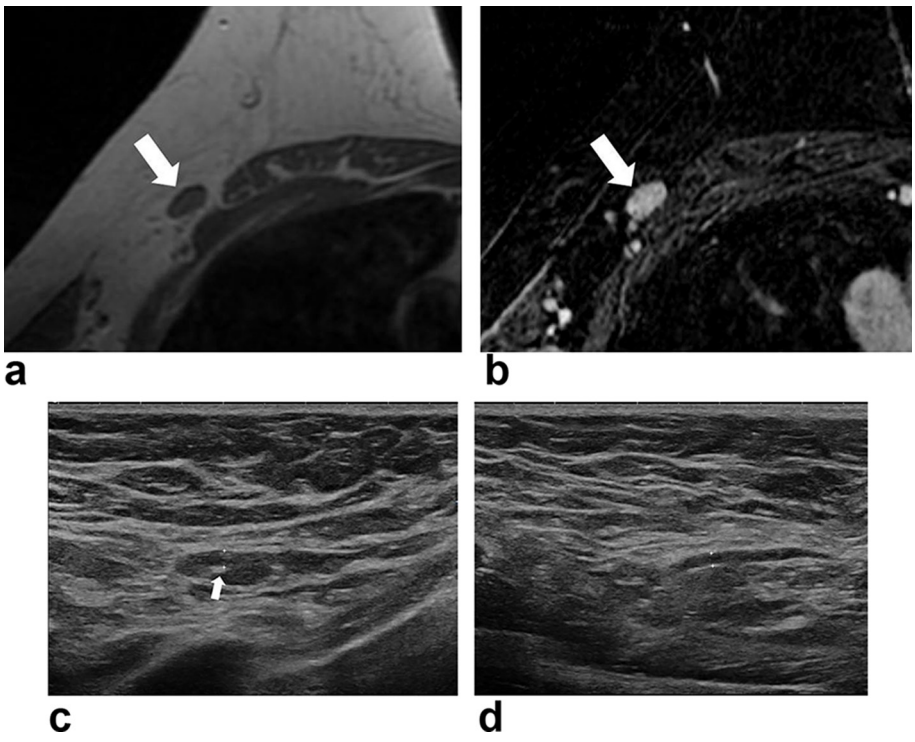

However, our current results, together with our previous results, suggest that SD in MRI may potentially indicate the presence of nodal metastases.[25] A previous study by Hyun et al used an SD exceeding 1 cm for ALN positivity in MRI, whereas our ROC analysis showed the optimum cut-off value of SD was >5.9 mm.[21]

Semantic features of ALN (eccentricity, fatty hilum loss, and irregularity) have been used for predicting nodal metastases in previous studies.[20,26] We found that eccentricity was significantly associated with nodal metastases in both ultrasound and MRI; thus, eccentricity appears to be useful as a criterion for further evaluation (*e.g.* aspiration, biopsy etc.). However, care should be taken to differentiate eccentricity from the irregularity or lobulation of the cortical contour. Fatty hilum loss is generally considered to be suggestive of nodal metastases. Theoretically, fatty hilum loss represents the replacement of fatty tissue with inflammatory or metastatic cells. Our study showed that fatty hilum loss had the strongest predictive value for nodal metastases with an adjusted OR of 27.2 in ultrasound. However, fatty hilum loss was interestingly not significantly associated with nodal metastases after adjusting for clinicopathological characteristics in MRI; it showed borderline significance in the unadjusted OR (p = .082). The lower resolution of an MRI may contribute to this finding because the very thin fatty tissue inside the ALN may be obscured in an MRI with a relatively high FOV (Figure 4). Irregularity, which is often adopted as criterion in some studies, appears to be unreliable, for our results did not show a significant association between irregularity and nodal metastases in both ultrasound and MRI. This may reflect the difficulty encountered in distinguishing normal lobulation from irregular changes of the cortex.

We acknowledge several limitations in our study. First, owing to it being a single-center retrospective analysis, the optimum criteria were not validated externally with different cohorts. However, our study involved large series of patients with breast cancers who underwent axillary surgery and fine measurement of CT with comparison of contralateral ALN; and the consecutive patients were prospectively collected. But future studies will be necessary to externally validate our results in a larger, multi-institutional patient cohort. Second, node-to-node analysis was not performed in our study, and not all patients in this study underwent ALND. The node analyzed, which was the most suspicious one, might not have been evaluated pathologically in patients who underwent SLNB.

In conclusion, among the quantitative features, all CT-derived parameters can be used for predicting nodal metastases. Significant predictors of semantic features were heterogeneous between ultrasound and MRI.

FUNDING

This research was supported by Basic Science Research Program through the National Research Foundation of Korea (NRF) funded by the Ministry of Education (NRF-2017R1D1A1B03032143).

REFERENCES

1. Krag D, Weaver D, Ashikaga T, Moffat F, Klimberg VS, Shriver C, et al. The sentinel node in breast cancer-a multicenter validation study. *N Engl J Med* 1998; **339**: 941–6. doi: https://doi.org/10.1056/NEJM199810013391401
2. Hieken TJ. The promise of axillary imaging in individualized surgical management of breast cancer patients: another step forward. *Ann Surg Oncol* 2014; **21**: 3369–71. doi: https://doi.org/10.1245/s10434-014-3853-9
3. Park SH, Kim MJ, Park BW, Moon HJ, Kwak JY, Kim EK. Impact of preoperative ultrasonography and fine-needle aspiration of axillary lymph nodes on surgical management of primary breast cancer. *Ann Surg Oncol* 2011; **18**: 738–44. doi: https://doi.org/10.1245/s10434-010-1347-y
4. del Riego J, Diaz-Ruiz MJ, Teixidó M, Ribé J, Vilagran M, Canales L, et al. The impact of preoperative axillary ultrasonography in T1 breast tumours. *Eur Radiol* 2016; **26**: 1073–81. doi: https://doi.org/10.1007/s00330-015-3901-2
5. Humphrey KL, Saksena MA, Freer PE, Smith BL, Rafferty EA. To do or not to do: axillary nodal evaluation after ACOSOG Z0011 trial. *Radiographics* 2014; **34**: 1807–16. doi: https://doi.org/10.1148/rg.347130141
6. Kim EJ, Kim SH, Kang BJ, Choi BG, Song BJ, Choi JJ. Diagnostic value of breast MRI for predicting metastatic axillary lymph nodes in breast cancer patients: diffusion-weighted MRI and conventional MRI. *Magn Reson Imaging* 2014; **32**: 1230–6. doi: https://doi.org/10.1016/j.mri.2014.07.001
7. Gentilini O, Veronesi U. Abandoning sentinel lymph node biopsy in early breast cancer? A new trial in progress at the European Institute of Oncology of Milan (SOUND: Sentinel node vs Observation after axillary UltraSouND). *Breast* 2012; **21**: 678–81. doi: https://doi.org/10.1016/j.breast.2012.06.013
8. Gentilini O, Botteri E, Dadda P, Sangalli C, Boccardo C, Peradze N, et al. Physical function of the upper limb after breast cancer surgery. Results from the SOUND (Sentinel node vs. Observation after axillary Ultra-souND) trial. *Eur J Surg Oncol* 2016; **42**: 685–9. doi: https://doi.org/10.1016/j.ejso.2016.01.020
9. Reimer T, Hartmann S, Stachs A, Gerber B. Local treatment of the axilla in early breast cancer: concepts from the national surgical adjuvant breast and bowel project B-04 to the planned intergroup sentinel mamma trial. *Breast Care* 2014; **9**: 1–95. doi: https://doi.org/10.1159/000360411
10. Reimer T, Stachs A, Nekljudova V, Loibl S, Hartmann S, Wolter K, et al. Restricted axillary staging in clinically and sonographically node-negative early invasive breast cancer (c/iT1-2) in the context of breast conserving therapy: first results following commencement of the Intergroup-Sentinel-Mamma (INSEMA) trial. *Geburtshilfe Frauenheilkd* 2017; **77**: 149–57. doi: https://doi.org/10.1055/s-0042-122853
11. Caudle AS, Hunt KK, Kuerer HM, Meric-Bernstam F, Lucci A, Bedrosian I, et al. Multidisciplinary considerations in the implementation of the findings from the American College of Surgeons Oncology

Group (ACOSOG) Z0011 study: a practice-changing trial. *Ann Surg Oncol* 2011; **18**: 2407–12. doi: https://doi.org/10.1245/s10434-011-1593-7

12. Lyman GH, Giuliano AE, Somerfield MR, Benson AB, Bodurka DC, Burstein HJ, 3rd BDC, et al. American Society of Clinical Oncology guideline recommendations for sentinel lymph node biopsy in early-stage breast cancer. *J Clin Oncol* 2005; **23**: 7703–20. doi: https://doi.org/10.1200/JCO.2005.08.001
13. Boughey JC. How do the AMAROS trial results change practice? *Lancet Oncol* 2014; **15**: 1280–1. doi: https://doi.org/10.1016/S1470-2045(14)71018-6
14. Allred DC, Harvey JM, Berardo M, Clark GM. Prognostic and predictive factors in breast cancer by immunohistochemical analysis. *Mod Pathol* 1998; **11**: 155–68.
15. Wolff AC, Hammond ME, Hicks DG, Dowsett M, McShane LM, Allison KH, et al. Recommendations for human epidermal growth factor receptor 2 testing in breast cancer: American Society of Clinical Oncology/College of American Pathologists clinical practice guideline update. *J Clin Oncol* 2013; **31**: 3997–4013. doi: https://doi.org/10.1200/JCO.2013.50.9984
16. Bedi DG, Krishnamurthy R, Krishnamurthy S, Edeiken BS, Le-Petross H, Fornage BD, et al. Cortical morphologic features of axillary lymph nodes as a predictor of metastasis in breast cancer: in vitro sonographic study. *AJR Am J Roentgenol* 2008; **191**: 646–52. doi: https://doi.org/10.2214/AJR.07.2460
17. Tateishi T, Machi J, Feleppa EJ, Oishi R, Furumoto N, McCarthy LJ, et al. In vitro B-mode ultrasonographic criteria for diagnosing axillary lymph node metastasis of breast cancer. *J Ultrasound Med* 1999; **18**: 349–56. doi: https://doi.org/10.7863/jum.1999.18.5.349
18. Grimm LJ, Viradia NK, Johnson KS. Normal axillary lymph node variability between white and black women on breast MRI. *Acad Radiol* 2018; **25**: 305–8. doi: https://doi.org/10.1016/j.acra.2017.10.007
19. Baltzer PA, Dietzel M, Burmeister HP, Zoubi R, Gajda M, Camara O, et al. Application of MR mammography beyond local staging: is there a potential to accurately assess axillary lymph nodes? evaluation of an extended protocol in an initial prospective study. *AJR Am J Roentgenol* 2011; **196**: W641–W647. doi: https://doi.org/10.2214/AJR.10.4889
20. Cho N, Moon WK, Han W, Park IA, Cho J, Noh DY. Preoperative sonographic classification of axillary lymph nodes in patients with breast cancer: node-to-node correlation with surgical histology and sentinel node biopsy results. *AJR Am J Roentgenol* 2009; **193**: 1731–7. doi: https://doi.org/10.2214/AJR.09.3122
21. Hyun SJ, Kim EK, Moon HJ, Yoon JH, Kim MJ. Preoperative axillary lymph node evaluation in breast cancer patients by breast magnetic resonance imaging (MRI): Can breast MRI exclude advanced nodal disease? *Eur Radiol* 2016; **26**: 3865–73. doi: https://doi.org/10.1007/s00330-016-4235-4
22. Mainiero MB, Cinelli CM, Koelliker SL, Graves TA, Chung MA. Axillary ultrasound and fine-needle aspiration in the preoperative evaluation of the breast cancer patient: an algorithm based on tumor size and lymph node appearance. *AJR Am J Roentgenol* 2010; **195**: 1261–7. doi: https://doi.org/10.2214/AJR.10.4414
23. Jackson RS, Mylander C, Rosman M, Andrade R, Sawyer K, Sanders T, et al. Normal axillary ultrasound excludes heavy nodal disease burden in patients with breast cancer. *Ann Surg Oncol* 2015; **22**: 3289–95. doi: https://doi.org/10.1245/s10434-015-4717-7
24. Le-Petross HT, McCall LM, Hunt KK, Mittendorf EA, Ahrendt GM, Wilke LG, et al. Axillary ultrasound identifies residual nodal disease after chemotherapy: results from the American College of Surgeons Oncology Group Z1071 trial (Alliance). *AJR Am J Roentgenol* 2018; **210**: 669–76. doi: https://doi.org/10.2214/AJR.17.18295
25. Kim WH, Lee SW, Kim HJ, Chae YS, Jeong SY, Jung JH, et al. Prediction of advanced axillary lymph node metastases (ypN2-3) using breast MR imaging and PET/CT after neoadjuvant chemotherapy in invasive ductal carcinoma patients. *Sci Rep* 2018; **8**: 3181. doi: https://doi.org/10.1038/s41598-018-21554-z
26. Alvarez S, Añorbe E, Alcorta P, López F, Alonso I, Cortés J. Role of sonography in the diagnosis of axillary lymph node metastases in breast cancer: a systematic review. *AJR Am J Roentgenol* 2006; **186**: 1342–8. doi: https://doi.org/10.2214/AJR.05.0936